

Effects of Talc on the Mechanical and Thermal Properties of Polylactide

Fengmei Yu, Tao Liu, Xiuli Zhao, Xuejiang Yu, Ai Lu, Jianhua Wang

Institute of Chemical Materials, China Academy of Engineering Physics, Mianyang 621900, People's Republic of China

Received 27 January 2011; accepted 3 October 2011

DOI 10.1002/app.36260

Published online in Wiley Online Library (wileyonlinelibrary.com).

ABSTRACT: Polylactide (PLA) composites with various talc content were prepared by melt extrusion. The thermal, dynamic mechanical, tensile and flexural properties, and fracture surface morphologies of neat PLA and PLA/talc composites were investigated and compared. The results showed that talc had significant nucleation effect and the cold crystallization temperature of PLA decreased with talc concentration. The thermal degradation and heat distortion temperature of PLA were slightly enhanced by compounding with talc. Talc showed significant reinforcing and toughening effects on PLA, the tensile strength, flexural strength and modulus increased with talc content ranging from 0 to 24.3 wt %. The results of tensile test

showed that the elongation at break increased with talc content up to 18.1 wt % with obvious changes in fracture behavior, changing from brittle to ductile, when talc content increased to 24.3%, samples failed in a brittle manner with low elongation at break. The fracture surface morphologies showed that the talc layers were partially delaminated, aligned along the flow direction, and uniformly dispersed in the PLA matrix. The results obtained by SEM and FTIR confirmed that the interfacial adhesion between talc and PLA matrix was good. © 2012 Wiley Periodicals, Inc. *J Appl Polym Sci* 000: 000–000, 2012

Key words: composites; polylactide; talc; crystallization

INTRODUCTION

Polymer materials have brought many benefits to mankind and enormous amounts and varieties of plastics such as polyolefin, polystyrene, are produced, consumed and discarded into the environment. Most of plastics made from petroleum are undegradable, the waste of them has led to serious environmental pollution. Therefore, there is an urgent need for developing biodegradable commodity polymers to replace the traditional petroleum plastics. PLA is a linear aliphatic thermoplastic polyester produced by the condensation polymerization of the lactic acid monomers or the ring-opening polymerization of lactides, which are obtained from the fermentation of renewable agricultural products such as corn, etc.¹ The final degradation products of PLA are CO₂ and H₂O which are completely innocuous to human and environment, thus there is an increasing interest in using PLA to replace undegradable polymer especially as packing materials. PLA has good mechanical properties, thermal plasticity and biocompatibility, and is readily fabri-

cated,² thus it is considered as the most promising biodegradable polymer. However, some properties such as strength, toughness, and heat distortion temperature (HDT) are not satisfactory for end use.

Preparing composites by compounding polymer with fillers has already been proved to be an effective way to improve properties of polymer, while it could reduce the production costs.³ Layered silicate fillers have large potential in improving the properties of polymer because its high aspect ratio, intercalated or exfoliated polymer/layered silicate nanocomposites with better properties than pristine polymer could be prepared by compounding them with polymer matrix.⁴ The effects of layered silicates such as montmorillonite, mica and saponite on HDT, dynamic mechanical, flexural, barrier properties, and biodegradability of PLA has been studied extensively.^{5–13} In addition to clay, talc is also a layer silicate mineral characterized by three octahedral Mg positions per four tetrahedral Si positions with the chemical formula Mg₃Si₄O₁₀(OH)₂,¹⁴ which is the softest mineral and its lamellar platelets are only held together by Van der Waals' force.¹⁵ One important difference between talc and clay such as montmorillonite is that talc is neutrally charged while the clay is negatively charged, which indicate that there are no interlayer metal cations in galleries of talc and it is difficult to be intercalated with long-chain organic compounds by ion exchange. Talc is difficult to disperse in water and considered to be hydrophobic and more compatible with polymer matrix,¹⁴

Correspondence to: J. Wang (wangjh_caep@163.com) and X. Zhao (zhaoxl75@163.com).

Contract grant sponsor: Science and technology foundation of China Academy of Engineering Physics; contract grant number: 2008A0302012.

which has been widely used as an effective filler in polymer, such as polyethylene,¹⁶ polystyrene,¹⁷ poly(vinyl chloride)¹⁸ and poly(3-hydroxybutyrate-co-3-hydroxyvalerate) composites,¹⁹ to improve their properties. Especially, there are many researches on the effect of talc on the mechanical properties, thermostability, crystallizability and rheology of polypropylene/talc composites.^{20–24} However, there are rarely published papers on the effect of talc on the properties of PLA except two recent papers.^{25,26} Huda et al. reported that the mechanical properties of PLA/recycled newspaper cellulose fibers composites were improved significantly by compounding with 10 wt % talc.²⁵ Angela et al. confirmed that talc exhibited strong nucleation effect and the isothermal crystallization halftimes of PLA decreased nearly 65-fold by the addition of only 2% talc.²⁶ However, almost no studies about the effect of talc on the mechanical properties of neat PLA have been reported.

To investigate the effect of talc on the properties of PLA, we prepared PLA/talc composites with various talc concentrations by melt extrusion, their thermal properties, mechanical properties, and fracture modes were studied and compared with those of neat PLA. The relationship between properties and talc concentration as well as the reinforcing and toughening effects of talc on PLA were identified.

EXPERIMENTAL

Materials

A commercial injection-grade PLA (Revo 201) was purchased from Zhejiang Hisaiv Biomaterials and used after being dried at 80°C for 12 h. The talc powder (2500 mesh, an average aspect ratio of 6 estimated by SEM) was purchased from Sichuan Serpentine Mineral Factory in China. 3-Aminopropyltriethoxysilane used as coupling agent in filler treatment was purchased from Nanjing Crompton Shuguang Organosilicon Specialties.

Filler treatment

The surface treatment of the talc was carried out in solution. First, the silane coupling agent was diluted in aqueous ethanol solution (a 95 wt % ethanol/5 wt % water solution), and then talc powder was added in the solution and the slurry was stirred by hand until all talc particles being wetted. For complete surface wetting, the following amounts were required per kilogram of talc: 3.0 g of silane diluted in 497.0 g of an aqueous ethanol solutions. After treatment, the filler was dried in an oven at 105°C for 24 h.

TABLE I
Composition of PLA/Talc Composites

Sample	PLA/wt %	Talc/wt %	KH550/ ^a wt %
Neat PLA	100	0	0.3
PLAT1	97.5	2.5	0.3
PLAT2	95	5.0	0.3
PLAT3	90	10	0.3
PLAT4	85	15	0.3
PLAT5	80	20	0.3
PLAT6	70	30	0.3
PLAT7	90	10 ^b	0

^a wt% with respect to the weight of PLA.

^b Untreated talc.

Sample preparation

To disperse talc powder well in PLA matrix, PLA was treated with silane coupling agent(0.3 wt % of PLA) by hand shaking PLA pellets and coupling agent in a bag firstly, then treated talc powder was added and mixed with treated PLA pellets in same manner, subsequently, the mixture was melt-extruded with a twin-screw extruder (Haake, PTW252). The extruder had eight controlled temperature zones which were set at 140, 150, 155, 160, 165, 150, 145, and 140°C, from the feeding zone to the die zone. The screw speed was maintained at 90 rpm for all runs. The compositions of each sample are presented in Table I. The extrudate was then pelletized and dried at 80°C for 24 h in a convection oven to remove water. Standard tensile (ISO 527-2) and flexural (ISO 178) specimens were prepared by injection molding with an injection molding machine (Chen Hsong, SM55EJ). The mold temperature and cooling time were set at 30°C and 45 s, respectively.

Talc content determination

As some talc filler might be lost during compounding process, a polymer burn-off test or ashing was performed to determine the final filler content in injection-molded specimens. Three injection-molded specimens for each sample were randomly selected and respectively burnt off in a furnace with the temperature set at 500°C. The residue was then weighed, and the corresponding average weight fraction of talc was calculated and listed in Table II.

Thermal properties

The crystallization behavior and melting characteristics of neat PLA and PLA/talc composites were studied by differential scanning calorimetry (DSC) (Perkin-Elmer, Diamond) in a nitrogen atmosphere at a heating and cooling rate of 10°C/min. The thermal stability of neat PLA and PLA/talc composites were studied by thermal gravimetric analysis with a

TABLE II
Characteristic Thermal Properties of PLA and PLA/Talc Nanocomposites

Sample	Talc (wt %)	T_g (°C)	T_{cc} (°C)	ΔH_{cc} (J/g)	T_m (°C)	ΔH_m (J/g)	X_c (%)	T_5 (°C)	T_{50} (°C)
Neat PLA	0	57.1	129.7	2.6	146.8	2.9	3.1	352.4	378.3
PLAT1	2.0	58.7	120.8	13.8	145.5	13.9	15.3	355.0	379.3
PLAT2	4.5	58.80	120.8	12.9	145.6	13.5	15.2	353.1	380.3
PLAT3	9.1	58.5	114.6	16.4	143.7	17.0	20.1	354.1	379.2
PLAT4	12.8	59.0	113.6	16.7	143.0	17.0	21.0	353.9	380.5
PLAT5	18.1	59.0	109.8	17.5	142.5	18.6	24.4	354.6	380.7
PLAT6	24.3	59.2	108.4	16.9	142.9	17.7	25.1	356.4	382.9

thermogravimetric analyzer (TA, TGA2050) in nitrogen atmosphere at a heating rate of 10°C/min from 30°C to 500°C. All specimens for DSC and TG analysis were cut from injection-molded samples, and at least one duplicate test was performed.

The HDT of neat PLA and PLA/talc composites were determined according to the standard ISO 75-1 and 75-2. The test specimens were loaded in three-point bending in the flatwise direction. A load of 0.45 MPa was placed on each specimen, and the temperature was increased at 2°C/min until the specimen deflect 0.32 mm, three replicates were tested for each sample. The specimens with a dimension of 80 × 10 × 4 mm³ were prepared by injection molding.

Dynamic mechanical analysis

Dynamic mechanical properties of PLA and PLA/talc composites were studied by dynamic mechanical analysis (DMA) (TA, Q800). DMA specimens were cut from injection-molded samples and tested in a single-cantilever bending mode at an oscillating amplitude of 3μm and a frequency of 1 Hz. The temperature range studied was from 25 to 150°C/min with a heating rate of 3°C/min. Two specimens were tested to check for reproductivity.

Mechanical properties

The tensile and flexural properties were measured with a universal testing machine (Instron, 5582-SP1376) according to standards ISO 527-1, 527-2 and ISO 178. For tensile tests, a crosshead speed of 5 mm/min and a 25-mm extensionmeter were used. For flexural tests, a three-point loading system was used, and the crosshead speed was 2 mm/min. All tests were carried out in an air-conditioned room at 25°C, and each measurement was repeated at least five times.

Scanning electron microscope

Fracture surfaces of tensile samples were observed with scanning electron microscope (KYKY, 2800). All

fracture surfaces were coated with a thin layer of gold before examination by SEM.

Fourier Transform Infrared Spectroscopy Analysis

Fourier transform infrared spectroscopy (FTIR) analyses were performed using a THERMO Nicolet 6700 spectrometer equipped with attenuated total reflection (ATR) sampling accessory. The spectra were recorded from 400 to 4000 cm⁻¹ with a resolution of 2 cm⁻¹ and 32 scans. All FTIR samples were cut from injection-molded specimens.

RESULTS AND DISCUSSION

Thermal properties

The crystallization rate of pure PLA is very slow and the crystallization half time is in the range of 17–45 min.²⁶ Talc is a strong nucleating agent in the process of polymer crystallization, Angela et al. co-workers found that the isothermal crystallization half time of PLA at 115°C were decreased nearly 65-fold by adding 2% talc.²⁶ In our work, we had studied the effect of talc concentration on the crystallization behavior of PLA by DSC. Figure 1 shows the DSC scan curves of neat PLA and PLA/talc

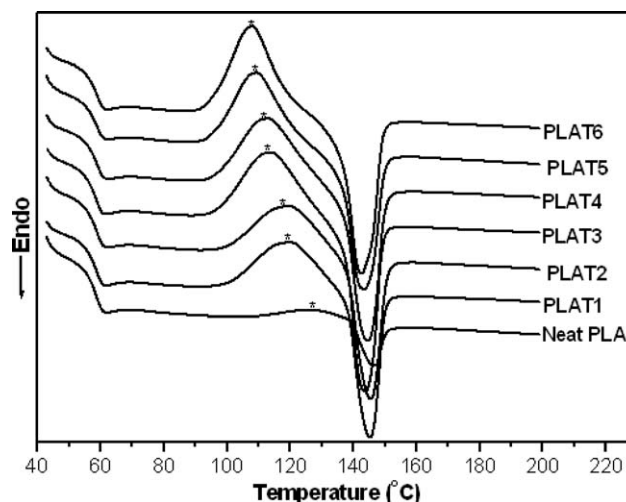


Figure 1 DSC curves of PLA and PLA/ talc composites in heating process.

composites in heating process. By considering the melting enthalpy of 100% crystalline polylactide as 93 J/g,²⁷ the crystallinity (χ_c) was calculated according to the following formula:

$$\chi_c = \frac{\Delta H_m}{(1 - \Phi) \times 93} \times 100\%$$

where ΔH_m is the melting enthalpy (in J/g) of sample and Φ is the weight fraction (in %) of talc in the composites. The DSC characteristic parameters are listed in Table II.

As expected, talc showed a strong nucleation effect since there are evident cold crystallization exotherm peaks in DSC curves of PLA/talc composites during heating, while the cold crystallization peak in DSC curve of neat PLA was unobvious. Figure 1 and Table II shows that the cold crystallization temperature (T_{cc}) decreased significantly with talc content increasing, and the T_{cc} of PLAT6 was lower than that of neat PLA by 21°C. Meanwhile, the crystallinity increased with talc content. The noticeable changes in T_{cc} and crystallinity suggested that the presence of talc improved the crystallization ability of PLA because of its strong nucleation effect. However, no crystallization peak was observed during cooling cycle at 10°C/min for all samples. This phenomenon suggested that crystalline nuclei formed during the cooling process have no enough time to grow, whereas they could reduce the crystallization induction period and increase the crystallization rate upon heating.²⁸ Furthermore, for each sample, we found that the enthalpy of cold crystallization (ΔH_{cc}) was very close to the enthalpy of melting (ΔH_m), which indicated that the injection-molded specimens were primarily amorphous.

From Table II, it can be seen that the addition of talc in PLA resulted in a increase in glass transition temperature (T_g) but decrease in melting temperature (T_m). The increase in T_g is attributed to the strong interfacial interaction between talc and PLA, which reduced the free volume and restricted the motion of PLA chains, thereby raising the T_g of PLA. The melting temperature decreased with the talc concentration, suggesting a larger number of less perfect crystals were nucleated at the talc particle surface and they can be melted in lower temperature.^{6,29,30}

Thermal stability of PLA and PLA/talc composites in nitrogen atmosphere were measured on TGA and the 5% loss temperature (T_5) and the 50% loss temperature (T_{50}) of all samples were listed in Table II. The results shows that the thermal degradation temperature of PLA/talc composites were slightly higher than that of neat PLA, we can infer that the talc filler have no marked effect on the thermal stability of PLA, and the increase of thermal degrada-

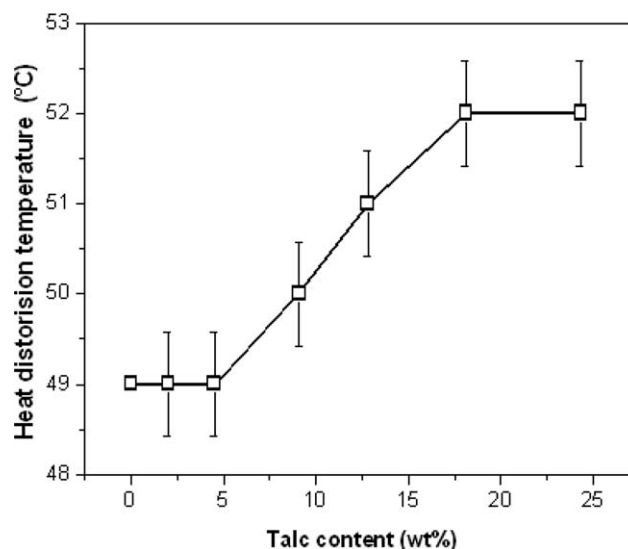


Figure 2 The HDT of neat PLA and PLA/talc composites.

tion temperature is mainly attributed to that talc filler dispersed in PLA matrix obstructed the diffusion of degradation products by creating a maze or tortuous path, consequently retarding the progress of degradation process.⁹

HDT is another important thermal property from the view of practical application, thus the HDT of neat PLA and PLA/talc composites were examined and compared. As seen in Figure 2, the talc filler has small effect on the HDT of PLA and the difference between the maximum and the minimum was only 3°. There was almost no change in HDT when the talc content was below 5 wt %, and above it the value of HDT increased linearly with talc content up to 18.1 wt %, thereafter the increase in talc content had no observable effect on the HDT of PLA/talc composites. The improvements in mechanical properties and crystallinity can result in the enhancement of HDT. Suprakas et al. reported that the HDT of PLA was enhanced significantly by compounding PLA with organically modified synthetic fluorine mica, when the injection-molded specimens were annealed at 120°C for 30 min to make PLA crystallize sufficiently.³¹ The results of DSC above show that injection-molded specimens in our work were primarily amorphous; hence, the increase in HDT of PLA/talc composites was due to the mechanical reinforcing effect of talc.

Dynamic mechanical properties

Figure 3(a) shows the temperature dependence of dynamic storage modulus of neat PLA and PLA / talc composites. Below T_g , the storage modulus of PLA/talc composites increased with the content of talc. The injection-molded specimens are mostly

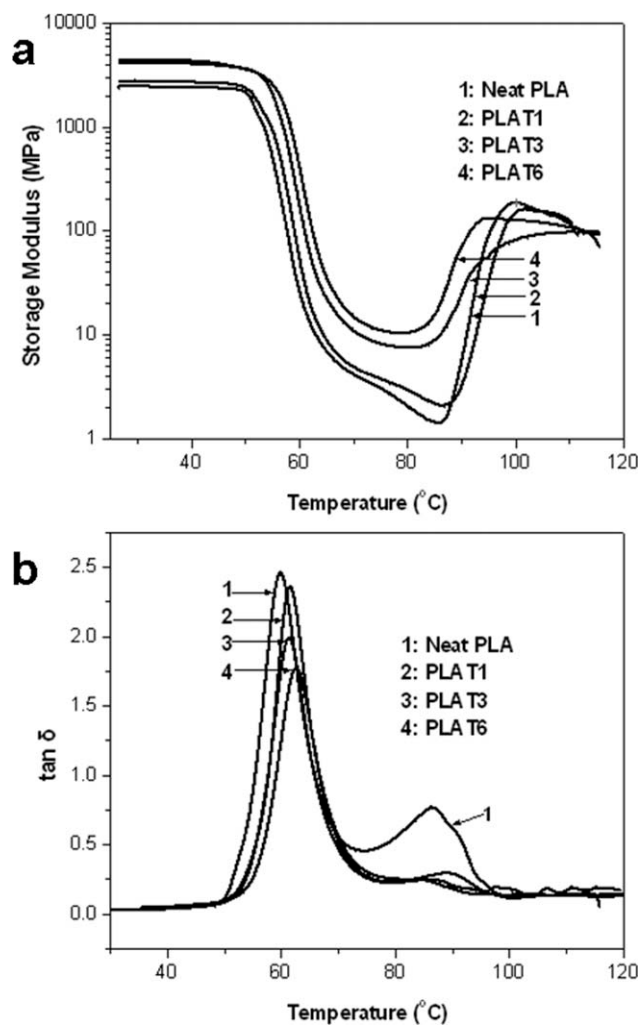


Figure 3 Temperature dependence of (a) storage modulus, and (b) $\tan \delta$ of PLA and PLA/talc composites.

amorphous identified by the DSC results; therefore, the enhancement in storage modulus is mainly attributed to the mechanical reinforcement effect of talc particles. At the temperature range of 60–90°C, the reinforcement effect of talc particles became more prominent, which indicate the PLA chains movement was restricted by the talc particles. It should be noted that the storage modulus of each sample increased when the temperature was above 90°C due to cold crystallization of PLA, but the storage modulus of neat PLA and PLAT1 are higher than that of PLAT3 and PLAT6. The initial cold crystallization temperature of PLAT3 and PLAT6 are 80.0°C and 78.2°C, obvious lower than 85.7°C of neat PLA, but there was almost no difference between neat PLA and PLAT1. It was somewhat different with the result obtained from DSC analysis at heating rate of 10°C/min, which indicate that low content talc have no significant nucleation effect and the crystallinity of PLA could not be increased by talc when the heating rate was slow.

Figure 3(b) shows the temperature dependence of loss factor ($\tan \delta$) of neat PLA and PLA/talc composites. The loss factor is sensitive to molecular motion and its peak represents the glass transition temperature. As shown in Figure 3(b), the T_g of PLA/talc composites was higher than that of neat PLA, which agreed with the results of DSC. Moreover, the maximal loss factor of PLA/talc composites were lower than that of neat PLA in glass transition region, and the difference between PLA/talc composites and neat PLA became more significant in cold crystallization region (75–95°C), which confirmed again that the PLA chains motion were restricted by talc particles due to the strong interfacial interaction.

Mechanical properties

The tensile stress–strain curves of neat PLA and PLA/talc composites and corresponding deformation characteristics are showed in Figures 4 and 5, which show that Talc had significant effect on the fracture behavior of PLA. Neat PLA exhibited the characteristics of brittle fracture behavior and fractured with lower elongation at break, meanwhile a few crazes were observed in the direction perpendicular to tensile stress without necking. The elongation at break increased with the talc content until 18.1 wt % and decreased at higher content as shown in Figure 6(a), simultaneously an obvious change in fracture mode was observed (shown in Fig. 5). For PLAT3, PLAT4, and PLAT5, samples failed with noted stress-whitening and necking phenomenon, which resulted in a higher elongation at break and the average were 3.2, 4.1, and 5.1%, respectively while the average of neat PLA was only 2.4%. Figure 6(b) shows the effect of talc content on the flexural

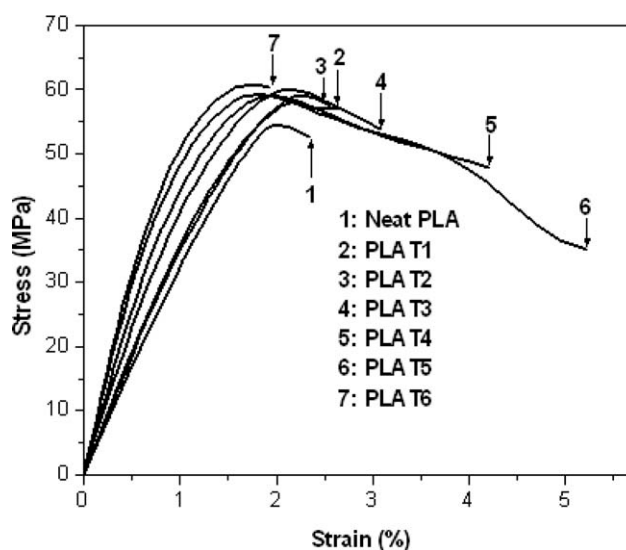


Figure 4 Tensile Stress-strain curves of neat PLA and PLA/talc composites.

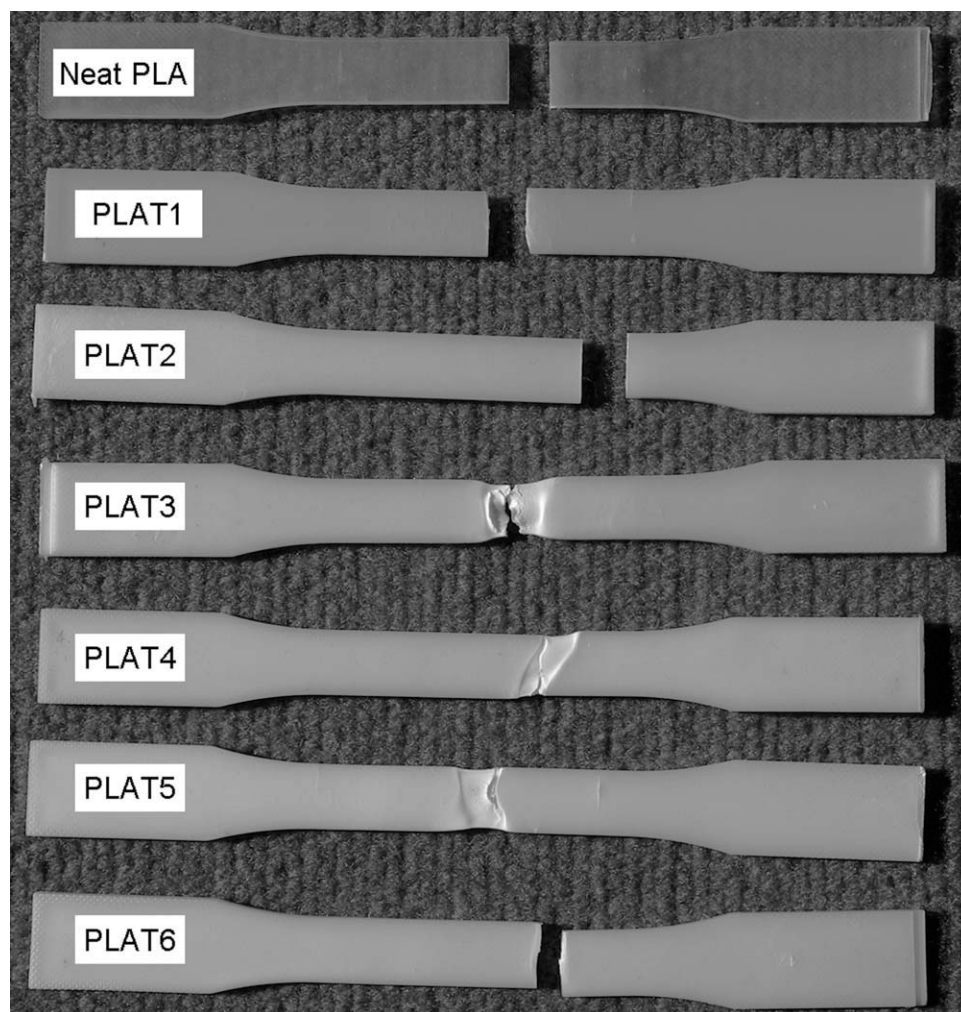


Figure 5 The photograph of specimens after tensile testing.

strength and modulus of PLA. From Figure 6, it can be observed that the tensile strength and flexural strength of PLA were enhanced evidently. It is worth noting that the enhancement of strength appeared in different magnitudes at various talc content ranges. At the talc content range of 0–2.0%, the strength increased significantly with the talc content increasing. Although the strength still increased with the talc content at the range of 2.0–24.3 wt %, the enhancement in strength was unobvious. Furthermore, the enhancement in flexural strength was more prominent than that in tensile strength. The flexural modulus was almost identical to the tensile modulus (not shown) and linearly increased with talc content, which was mainly attributed to the replacement of PLA by the more rigid talc particles as well as the talc filler restricting the mobility and deformability of the matrix.

The difference between neat PLA and its composites in mechanical properties and the failure characteristic suggested that talc has evident reinforcing and toughening effect on PLA. Talc has significant

reinforcing effect on polymer which was confirmed in many studies. Leong et al. reported that the tensile strength, flexural strength, and modulus of PP were improved obviously but the impact strength and the elongation at break decreased with talc loading.²⁰ Similar conclusions were deduced by Hamed et al.^{15,22,32} However, there are rarely reports on the strength and toughness of polymer were improved simultaneously by compounding with talc.

Morphology of fracture surfaces

To explore the reinforcing and toughening mechanism, the fracture surfaces after tensile testing as well as the cryo-fracture surfaces were observed by SEM. Figure 7 shows SEM micrographs of cryo-fracture surfaces. As shown in Figure 7, it is clear that talc layers are aligned along the injection flow direction and dispersed uniformly in the PLA matrix. There are no obvious aggregates but some thicker talc particles [indicated by circles in Fig. 7(e,f)] in SEM micrographs of PLAT5 and PLAT6. In addition,

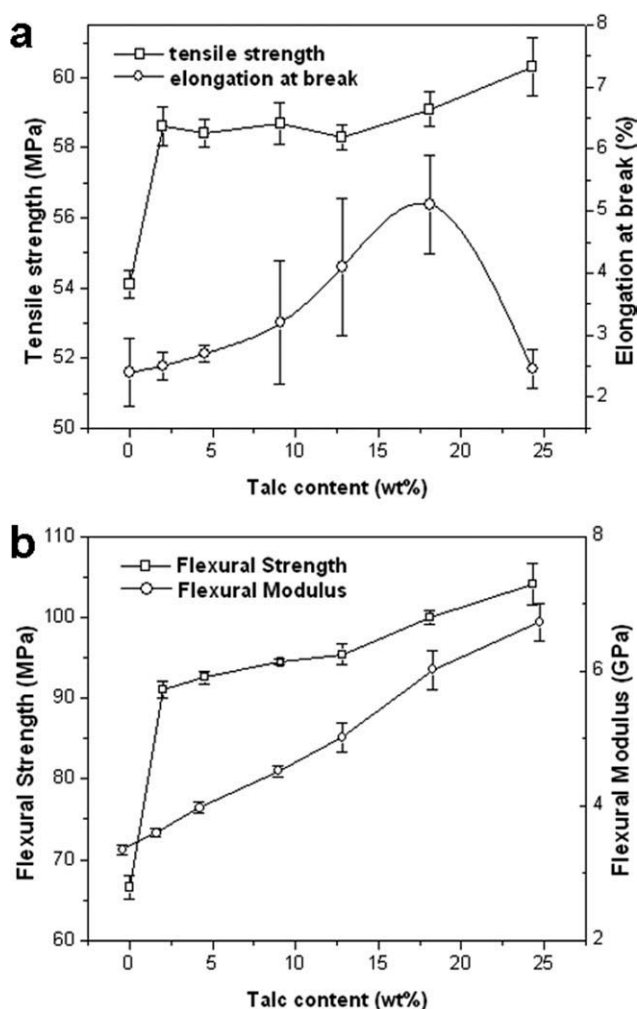


Figure 6 Mechanical properties of neat PLA and PLA/talc composites: (a) Tensile properties and (b) flexural properties.

the orientation direction of some talc layers [indicated by black arrows in Fig. 7(f)] was not parallel with the injection direction in PLAT6. It is worth noting that some voids can be seen in SEM micrographs of all PLA/talc composites except for PLAT1, and the number and width of these voids increased with the talc content increasing. These voids could be induced by debonding of talc particles from PLA matrix because of poor adhesion, or shelling of the middle talc layers. From the morphology of interface shown in Figure 8(h), we are able to infer that the interfacial adhesion is good; therefore, the shelling of the middle talc layers is the main reason inducing voids. It is well-known that the interlayer interaction of talc is weak and the lamellar platelets are only held together by Van der Waals' force, therefore some talc layers could be delaminated by shear force during compounding.³³ The extent of delamination decreased with talc content increasing, thereby the voids became more and wider, meanwhile some thicker talc particles occurred in composites with

higher talc content. The extent of delamination is responsible for the different reinforcing effect of talc at various talc content ranges. When the talc content is lower, most of talc particles could be delaminated to thinner flakes and the strength increased significantly. The extent of delamination, that is, the interfacial area did not increase linearly with the talc content increasing after a critical content and more thicker talc particles dispersed in composites, therefore the enhancement in strength increased slowly with talc content increasing.

On the basis of the above evidence, we can conclude that the improvements in tensile and flexural strength were mainly attributed to good adhesion between PLA matrix and talc as well as the platy or flaky nature of talc. Because of platy nature, talc has high aspect ratio which increased the interfacial area and interaction between it with PLA matrix. Strong interfacial interactions increased stress transfer to the fillers from polymer matrix during external loading,^{20,34} resulting in high strength of the PLA/talc composites. On the other hand, the talc layers could be aligned along the polymer flow direction and dispersed in polymer matrix more uniformly,³⁵ which also makes talc be a stronger reinforcing filler. The external loading direction and the orientation direction of talc are parallel in tensile test but perpendicular in flexural test, therefore talc show different reinforcing effect on tensile and flexural strength. Talc layers are easy to slip during tensile testing, resulting the enhancement in tensile strength is lower than that of flexural strength.

The increase in elongation at break and the change in failure mode showed that talc has significant toughening effect. Massive crazing and shearing yield are two toughening mechanisms of polymers. For rigid particulate fillers toughening polymer composites, debonding at the filler surface can induce massive crazing, and/or shear yielding if the plastic resistance of the matrix is decreased to below the applied stress due to the release of strain constraints.^{36,37} The platy nature of talc led to large interfacial area between the talc and PLA. Therefore, debonding at the talc surface would induce massive crazes which showed as significant stress-whitening during tensile testing. Significant strain softening phenomena and shear deformation bands were observed from Figures 4 and 5, which suggested the occurrence of shear yielding. Namely, talc particles induced PLA matrix around them producing microcracks so as to release the constraints for shear yielding, and to a large extent, they can prevent the microcracks from propagating into catastrophic cracks and result in high elongation at break. On the other hand, that the orientation direction of talc layers is coincide with the tensile direction made toughening effect of talc more significant, because

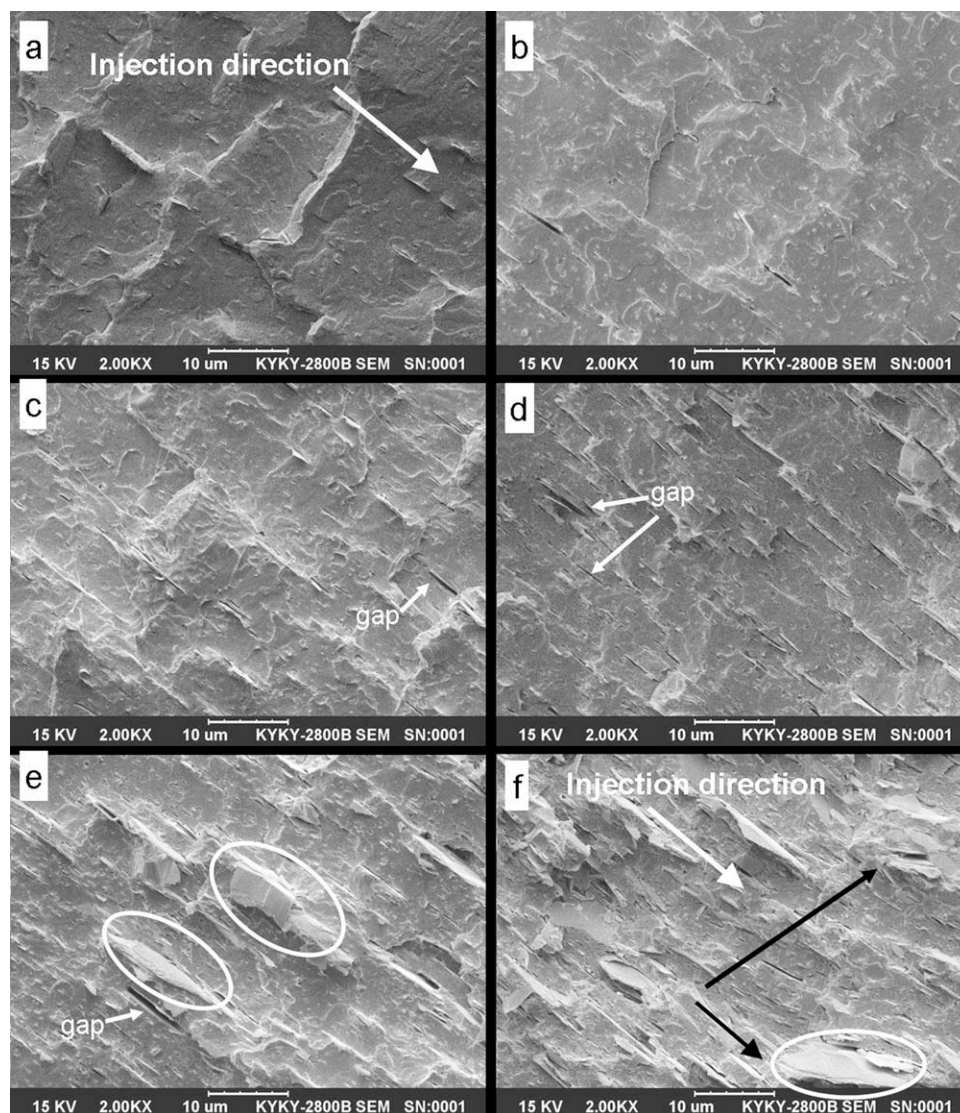


Figure 7 SEM micrographs of the cryo-fractured surfaces of PLA/talc composites: (a) PLAT1, (b) PLAT2, (c) PLAT3, (d) PLAT4, (e) PLAT5, (f) PLAT6.

the lamellar platelets of talc are only held together by Van der Waals' force and easy to slip under uniaxial tension, which is benefit of to induce shear yielding. In addition, these orientated talc layers along tensile direction could prevent more effectively microcracks from propagating along fracture direction.

When the talc content was increased from 18.1 to 24.3%, the tensile strength of PLAT6 was slightly higher than that of PLAT5, however the elongation at break was dramatically decreased from 5.1 to 2.5%, and the fracture mode changed from ductile behavior to brittle behavior (shown in Fig. 5). This could be attributed to that the high talc content led to insufficient delamination and appearance of many thicker talc particles, which acted as material flaws and triggered brittle fracture in the tensile testing. Another important factor is that the talc orientation

degree decreased and the orientation direction of some talc layers were not parallel with the injection or tensile direction when the talc content was 24.3 wt % [shown in Fig. 7(f)], which is disadvantageous to prevent the propagating of microcracks along the fracture direction.

The deduction about toughening mechanisms can be confirmed by results of fracture surface morphologies of samples after tensile testing. As shown in Figure 8(a), matching its brittle fracture behavior, neat PLA exhibited a fairly smooth fracture surface because of lacking large scale of plastic deformation. Figure 8(b,c) are fracture surface morphologies of PLAT1 and PLAT2, respectively. The fracture surfaces are slightly rougher than that of neat PLA and talc particles are clearly visible and well dispersed in PLA matrix. From the photographs, only a few fibrils can be observed and the failure modes of

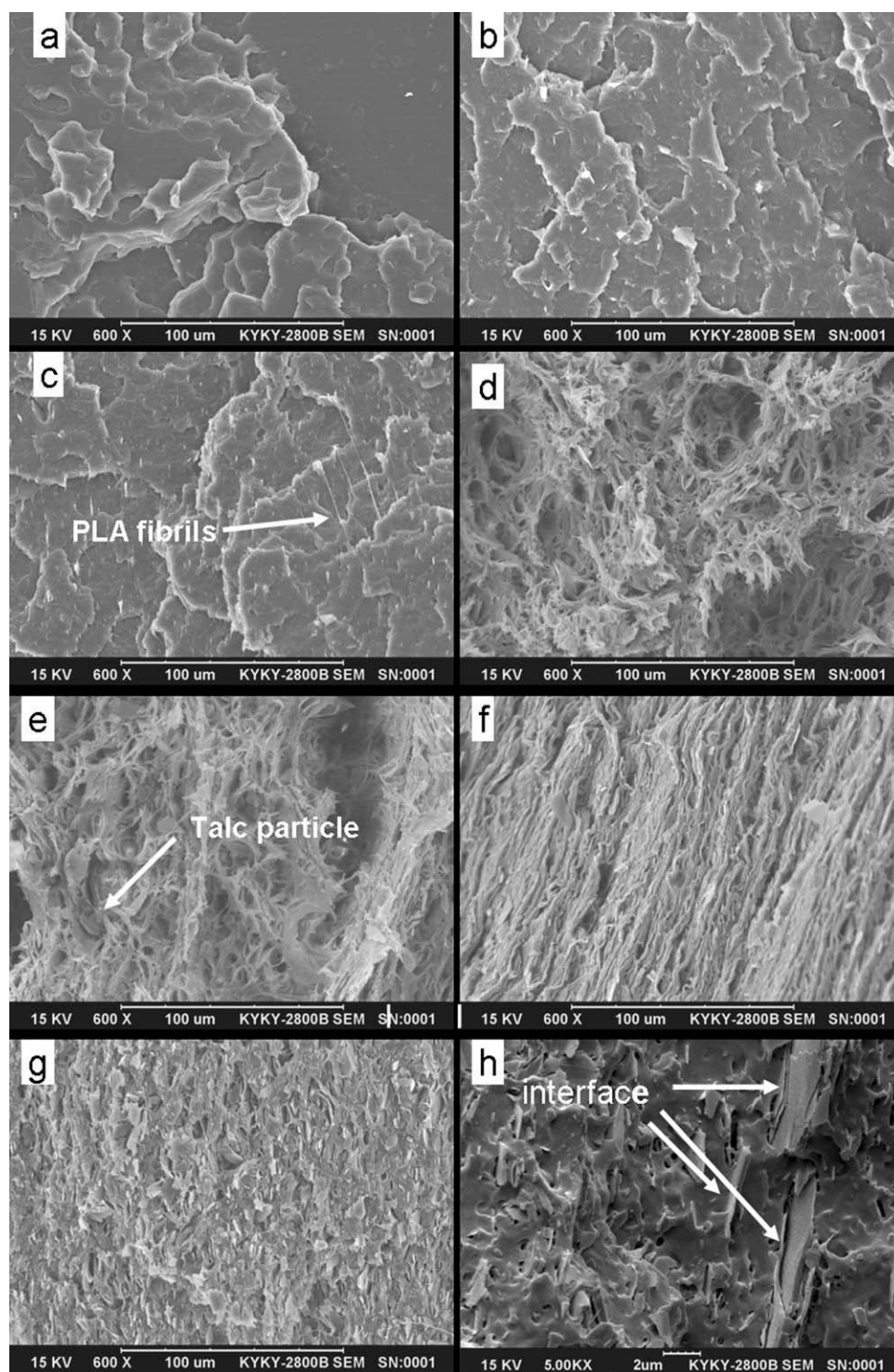


Figure 8 SEM micrographs of the fracture surfaces of tensile specimens: (a) neat PLA, (b) PLAT1, (c) PLAT2, (d) PLAT3, (e) PLAT4, (f) PLAT5, (g) PLAT6 at magnification of 600 and (h) PLAT6 at magnification of 5000.

these two specimens showed as typical brittle fracture similarly to neat PLA.

When the talc content increased further, the fracture surfaces changed markedly [shown in Fig. 8(d,e)] and exhibited ductile fracture surface morphology, numerous fibrils were drawn out of the matrix producing a large amount of cavities and a

few talc particles can be observed. The cavities were microvoids which initiated ligament shear yielding process during the tension.³⁴ Characteristics showed in Figure 8(d,e) indicated that large scale of plastic deformation was produced before specimens failure which is responsible for the necking phenomena and increase of elongation at break.

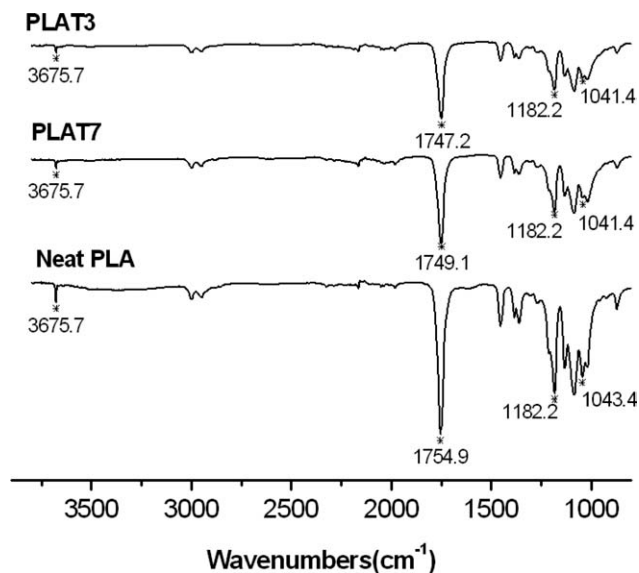


Figure 9 FTIR spectra of PLA, PLAT3, and PLAT7.

In fracture face of PLAT5 as shown in Figure 8(f), the fibrils is less than that of PLAT3 and PLAT4, but many cracks perpendicular to tensile direction can be observed clearly, which is the result of the propagation of massive microcracks which mainly induced by the debonding at the PLA/talc interface during tensile process. Forming of massive microcracks or microvoids can absorb much energy, meanwhile the presence of talc particles can prevent propagation of cracks and retard material failure; therefore, the specimens of PLAT5 still behaved as ductile fracture with high elongation at break.

Figure 8(g) shows that the fracture face of PLAT6 is very rough and there are lots of talc platelets or particles. As mentioned above, the high concentration of talc led to decrease of delamination degree and appearance of thicker talc particles, which acted as a stress concentration points or weak points and resulted brittle fracture behavior and lower elongation at break.

The role of coupling agent

γ -Aminopropyltriethoxysilane is a common coupling agent and can condense on the surface of talc during drying process.³⁸ The effect of silane coupling agent on the interfacial adhesion between talc and PLA matrix was investigated by FTIR. Figure 9 presents the FTIR spectra of PLA and its composites. The peaks at 3675.7, 1754.9, 1182.2, and 1043.4 cm^{-1} were assigned to the stretching of O—H and C=O, anti-symmetrical and symmetrical stretching of C—O, respectively. Comparing with neat PLA, the absorption peaks of C=O stretching and C—O antisymmetrical stretching of PLAT3 as well as that of PLAT7 without silane coupling agent shifted to lower wave-

numbers, suggesting that there are strong interactions between PLA and talc filler probably due to hydrogen bonds formed between C=O of PLA and O—H of talc or N—H of silane coupling agent, which contribute to good interfacial adhesion in PLA/talc composites. The absorption frequency of C=O in PLAT3 is lower than that of C=O in PLAT7, suggesting that the interfacial interaction between PLA and talc was intensified by silane coupling agent.

CONCLUSION

PLA/talc composites were prepared by melt compounding using a twin-screw extruder and injection-molded into test specimens. Talc has significant nucleation effect and the cold crystallization decreased with talc content increasing; however, the injection-molded specimens of PLA/talc composites are still amorphous because of melt of all specimens experienced a fast cooling process in injection molding. The introduction of talc had inapparent improvements in thermal stability and thermal distortion temperature. Talc layers were aligned along the injection flow direction and dispersed uniformly in the PLA matrix. Talc has significant reinforcing effect and toughening effect, and the reinforcing effect of talc particles could be mainly attributed to the good interfacial adhesion between PLA matrix and the orientation of talc layers during processing. Characteristics of fracture surface of tensile specimens shown in SEM photographs suggested that interfacial debonding of PLA/talc composite can induce massive crazing, meanwhile talc particles diffused in PLA matrix can prevent the void coalescence and propagation of the crazes, which increase the toughness of PLA. Additionally, talc layers aligned along the tensile direction make its toughening effect on PLA more significant in tensile test because they are more advantageous to induce shear yielding and prevent microcracks from propagating along fracture direction. Thicker talc particles appeared in composites with higher talc content act as a stress concentration points or weak points and resulted poor toughness of PLA/talc composites.

References

1. James, L. *Polym Degrad Stab* 1998, 59, 145.
2. Suprakas, S. R.; Kazunobu, Y.; Akinobu, O.; Masami, O.; Kazue, U. *Macromol Rapid Commun* 2002, 23, 943.
3. Viera, K.; Joe, H.; Ivica, J.; Vasilij, S. *Polym Test* 1999, 18, 501.
4. Suprakas, S. R.; Masami, O. *Prog Polym Sci* 2003, 28, 1539.
5. Suprakas, S. R.; Pralay, M.; Masami, O.; Kazunobu, Y.; Kazue, U. *Macromolecules* 2002, 35, 3104.
6. Suprakas, S. R.; Masami, O. *Macromol Rapid Commun* 2003, 24, 815.
7. Pralay, M.; Kazunobu, Y.; Masami, O.; Kazue, U.; Kazuaki, O. *Chem Mater* 2002, 14, 4654.
8. Pluta, M.; Jeszka, J. K.; Boiteux, G. *Eur Polym J* 2007, 43, 2819.

9. Pluta, M.; Galeski, A.; Alexandre, M.; Paul, M. A.; Dubois, P. *J Appl Polym Sci* 2002, 86, 1497.
10. Mirosław, P. *J Polym Sci Part B: Polym Phys* 2006, 44, 3392.
11. Vahik, K.; Darrin, J. P. D. *Chem Mater* 2003, 15, 4317.
12. Jin-Hae, C.; Yeong, U. K.; Donghwan, C.; Emmanuel, P. G. *Polymer* 2003, 44, 3715.
13. Shu-Ying, G.; Jie, R.; Bo, D. *J Polym Sci Part B: Polym Phys* 2007, 45, 3189.
14. Zbik, M.; Smart, R. S. C. *Miner Eng* 2002, 154, 277.
15. Lubomir, L. J.; Pavlina, J.; Barbora, L.; Richard, T.; Richard, G.; Neil, R. *J Appl Polym Sci* 2008, 110, 2742.
16. Nanchun, C.; Lei, M.; Tao, Z. *Rare Metals* 2006, 25, 422.
17. Kwang, J. K.; James, L. W. *Polym Eng Sci* 1999, 39, 2189.
18. Xie, X. L.; Li, B. G.; Pan, Z. R.; Tjong, S. C. *J Appl Polym Sci* 2001, 80, 2105.
19. Audrey, W.; Bhardwai, R.; Amar, K. M. *Ind Eng Chem Res* 2006, 45, 7497.
20. Leong, Y. W.; Bakar, M. B. A.; Ishak, Z. A. M.; Ariffin, A.; Pukanszky, B. *J Appl Polym Sci* 2004, 91, 3315.
21. Leong, Y. W.; Ishak, Z. A. M.; Ariffin, A. *J Appl Polym Sci* 2004, 91, 3327.
22. Hamed, A.; Jalal, F. *Polym Compos* 2009, 30, 1743.
23. Shelesh-Nezhad, K.; Taghizadeh, A. *Polym Eng Sci* 2007, 47, 2124.
24. Yousef, J. *J Vinyl Addit Technol* 2010, 16, 70.
25. Huda, M. S.; Drzal, L. T.; Mohanty, A. K.; Misra, M. *Compos Part B-Eng* 2007, 38, 367.
26. Angela, M. H.; Ellen, C. *J Appl Polym Sci* 2008, 107, 2246.
27. Fisher, E. W.; Sterzel, H. J.; Wegner, G.; Kolloid, Z. Z. *Polym* 1973, 25, 980.
28. Hongbo, L.; Michel, A. H. *Polymer* 2007, 48, 6855.
29. Vahik, K.; Darrin, J. P. *Macromolecules* 2004, 37, 6480.
30. Joo, Y. N.; Suprakas, S. R.; Masami, O. *Macromolecules* 2003, 36, 7126.
31. Suprakas, S. R.; Kazunobu, Y.; Masami, O.; Akinobu, O.; Kazue, U. *Chem Mater* 2003, 15, 1456.
32. Guerrica-Echevarría, G.; Eguízaábal, J. I.; Nazaábal, J. *Eur Polym J* 1998, 34, 1213.
33. Weiguo, S.; Qi, W.; Kanshe, L. *Polym Eng Sci* 2005, 45, 451.2005.
34. Long, J.; Jinwen, Z.; Michael, P. W. *Polymer* 2007, 48, 7632.
35. Xing-Ping, Z.; Xiao-Lin, X.; Zhong-Zhen, Y.; Yiu-Wing, M. *Polymer* 2007, 48, 3555.
36. Gupta, M.; Lin, Y.; Deans, T.; Baer, E.; Hiltner, A.; Schiraldi, D. A. *Macromolecules* 2010, 43, 4230.
37. Kinloch, A. J. *Adv Polym Sci* 1985, 72, 45.
38. Leong, Y. W.; Abubakar, M. B.; Ishak, Z. A. M.; Ariffin, A. *J Appl Polym Sci* 2005, 98, 413.